A β Cephei pulsator and a changing orbital inclination in the high-mass eclipsing binary system VV Orionis

Southworth, John; Bowman, D M; Pavlovski, Krešimir

Source / Izvornik: **Monthly Notices of the Royal Astronomical Society: Letters, 2021, 501, L65 - L70**

Journal article, Published version
Rad u časopisu, Objavljena verzija rada (izdavačev PDF)

https://doi.org/10.1093/mnrasl/slaa197

Permanent link / Trajna poveznica: https://urn.nsk.hr/urn:nbn:hr:217:781795

Monthly Notices
of the
ROYAL ASTRONOMICAL SOCIETY

MNRAS **501,** L65–L70 (2021)
Advance Access publication 2020 December 16

doi:10.1093/mnrasl/slaa197

A β Cephei pulsator and a changing orbital inclination in the high-mass eclipsing binary system VV Orionis

John Southworth [1]★ D. M. Bowman [2] and K. Pavlovski[3]

[1]*Astrophysics Group, Keele University, Staffordshire ST5 5BG, UK*
[2]*Institute of Astronomy, KU Leuven, Celestijnenlaan 200D, B-3001 Leuven, Belgium*
[3]*Department of Physics, Faculty of Science, University of Zagreb, Bijenicka cesta 32, 10000 Zagreb, Croatia*

Accepted 2020 December 7. Received 2020 November 27; in original form 2020 July 10

ABSTRACT

We present an analysis of the high-mass eclipsing binary system VV Ori based on photometry from the *TESS* satellite. The primary star (B1 V, 9.5 $M_\odot$) shows β Cephei pulsations and the secondary (B7 V, 3.8 $M_\odot$) is possibly a slowly pulsating B star. We detect 51 significant oscillation frequencies, including two multiplets with separations equal to the orbital frequency, indicating that the pulsations are tidally perturbed. We analyse the *TESS* light curve and published radial velocities to determine the physical properties of the system. Both stars are only the second of their pulsation type with a precisely measured mass. The orbital inclination is also currently decreasing, likely due to gravitational interactions with a third body.

Key words: stars: binaries: eclipsing – stars: fundamental parameters – stars: oscillations.

1 INTRODUCTION

The study of eclipsing binary systems (EBs) is our primary source of empirical measurements of the masses and radii of normal stars (Andersen 1991; Torres, Andersen & Giménez 2010). From light and radial velocity (RV) curves, the masses and radii can be determined to high precision and accuracy (reaching 0.2 per cent; see Maxted et al. 2020), then used to check and calibrate theoretical models (e.g. Claret & Torres 2018; Tkachenko et al. 2020) or as distance indicators (e.g. Pietrzyński et al. 2019). Massive EBs are of particular interest because massive stars ($\gtrsim$8 $M_\odot$) have high multiplicity (Sana et al. 2012) and are important drivers in the chemical and dynamical evolution of galaxies (Langer 2012). However, a detailed understanding of their interior rotation and angular momentum transport mechanisms remains elusive (Aerts, Mathis & Rogers 2019).

Another method to constrain the properties of massive stars is via asteroseismology (Aerts, Christensen-Dalsgaard & Kurtz 2010). Each pulsation mode in a star is sensitive to a specific pulsation cavity, so multiperiodic pulsations are excellent tracers of the properties of stellar interiors (e.g. Aerts et al. 2003; Briquet et al. 2007, 2013). Two classes of massive pulsators are the β Cephei stars (Lesh & Aizenman 1978) and the slowly pulsating B-type (SPB) stars (Waelkens 1991). The pulsations in β Cephei stars are gravity (g) and pressure (p) modes of low radial order, are found in dwarfs and giants of mass 8–15 $M_\odot$, and have amplitudes up to a few tenths of a magnitude and pulsation periods of approximately 2–6 h (Stankov & Handler 2005). SPB pulsations occur in stars of roughly 3–9 $M_\odot$ and are high-order g modes with observationally challenging periods of 1–4 d. Space-based observations have recently revealed p- and g-mode pulsations in many massive stars above their canonical mass regimes, and demonstrated the diverse nature of variability for early-type stars (Pedersen et al. 2019; Burssens et al. 2020).

A promising avenue for constraining the interior physics in massive stars is to study pulsating stars in EBs, as this permits the confrontation of theoretical predictions with observed pulsation periods for stars of known mass and radius. Although several β Cephei stars in EBs are known (see Ratajczak, Pigulski & Pavlovski 2017), so far only one has a precisely measured mass and radius: V453 Cyg A (Southworth et al. 2020). SPB stars in EBs are even rarer: only one has been characterized in detail (V539 Ara; Clausen 1996) and no other examples are known. An important characteristic of binary stars is that tidal effects in eccentric systems may drive (Welsh et al. 2011; Hambleton et al. 2013; Fuller 2017) or perturb (Bowman et al. 2019; Fuller et al. 2020; Handler et al. 2020; Kurtz et al. 2020) pulsations.

VV Ori contains components of spectral types B1 V and B7 V in a circular orbit of period 1.485 d. Its eclipsing nature was discovered by Barr in 1903 (Barr 1905) and the early history of its study has been summarized by Wood (1946) and Duerbeck (1975). The two most recent studies of the system, Sarma & Vivekananda Rao (1995) and Terrell, Munari & Siviero (2007, hereafter T07), were the first to reliably determine its physical properties.

The multiplicity of the VV Ori system is not well established. The excess scatter seen in early RVs led to reluctant suggestions of a third body with an orbital period of 120 d (Daniel 1916; Struve & Luyten 1949), a finding that has not been substantiated (T07; Van Hamme & Wilson 2007). Horch et al. (2017) resolved a companion at an angular separation of 0.23 arcsec using speckle

★ E-mail: astro.js@keele.ac.uk

interferometry. The magnitude differences between this companion and the binary system are 3.88 mag at 692 nm and 3.43 mag at 880 nm. At a distance of 377 ± 31 pc (Gaia Collaboration 2018), this corresponds to a physical separation of 87 au and thus a minimum orbital period of about 180 yr. The resolved companion cannot therefore be responsible for the putative 120 d orbital variations.

2 OBSERVATIONS

VV Ori was observed using the NASA *TESS* satellite (Ricker et al. 2015). *TESS* is currently observing the majority of the sky, with each hemisphere divided up into 13 sectors based on ecliptic longitude. Observations in each sector last for 27.4 d, with an interruption for data download near the mid-point. VV Ori was observed in Sector 6 (2018 December 11–2019 January 07) and is scheduled to be re-observed in Sector 32 (2020 November 19–2020 December 17). The Sector 6 data were acquired at a cadence of 2 min, which are made available through the Mikulski Archive for Space Telescope portal, and yield a Nyquist frequency of 359.7 d^{-1}. Fig. 1 shows the simple aperture photometry light curve (Jenkins et al. 2016) of VV Ori.

3 LIGHT-CURVE ANALYSIS

The *TESS* light curve of VV Ori was first modelled using the JKTEBOP code in order to remove the signals of binarity (see Fig. 1). We used the orbital ephemeris from this fit to phase-bin the *TESS* data into 300 data points. The binned data were then analysed using the 2004 version of the WILSON–DEVINNEY code, which represents the stars using Roche geometry (hereafter WD2004; Wilson & Devinney 1971), driven by the JKTWD wrapper (Southworth et al. 2011). We fitted separately for the light produced by the two stars, the 'third light' from additional star(s) in the system, the potentials of the two eclipsing stars, and the orbital inclination. We did not fit for the effective temperatures ($T_{\rm eff}$ values) directly because the *TESS* passband is not implemented in the WD code. Limb darkening was included using the square-root law, with coefficients fixed to values from the tables of Van Hamme (1993). Fitting for the coefficients did not improve the quality of the fit. We searched for the possibility of an eccentric orbit but found no combination of eccentricity or argument of periastron that improved the fit compared to the assumption of a circular orbit. We adopted a mass ratio of 0.376 from T07.

The adopted model is given in Table 1 and plotted in Fig. 2, where the residuals come primarily from incomplete removal of the pulsations. Because the photon noise in the photometry is negligible, the uncertainties in the fitted parameters are dominated by choices made in the modelling process. We sought to capture these by quantifying the change in fitted parameter values between the adopted model and a range of alternative models with different values or treatments of albedo, stellar rotation rate, gravity darkening, limb darkening law, limb darkening coefficients, the reflection effect, numerical precision, and mass ratio. All uncertainties in Table 1 are the quadrature addition of the differences in parameters for each alternative model versus the adopted model, and are much larger than the formal errors computed by WD2004.

4 PHYSICAL PROPERTIES

Determination of the physical properties of VV Ori requires combining the results of the light-curve analysis with spectroscopic measurements of the $T_{\rm eff}$ values and velocity amplitudes (K_1 and K_2) of the two stars. For $T_{\rm eff}$, we adopted the values given by T07 and assigned a conservative uncertainty of ± 1000 K. Improved estimates of the $T_{\rm eff}$ values would be helpful in future.

RVs were measured by T07, who determined the stellar masses but not velocity amplitudes. We therefore fitted the RVs with JKTEBOP to determine $K_1 = 126.2 \pm 1.8\,{\rm km\,s^{-1}}$ and $K_2 = 316.4 \pm 6.5\,{\rm km\,s^{-1}}$. These uncertainties were calculated using Monte Carlo simulations (Southworth 2008) and with data errors estimated from the scatter around the best fit. Under the assumption that the orbital inclination decreased by $0.200 \pm 0.013^\circ\,{\rm yr^{-1}}$ in recent years (see below), K_1 and K_2 should be multiplied by a factor of $(\frac{\sin i_{2018}}{\sin i_{2005}})^3 = 0.979 \pm 0.002$ to correct them from the mean epoch of the spectra to that of the *TESS* data. The velocity amplitudes at the epoch of the *TESS* observations are therefore $K_1 = 123.5 \pm 2.0\,{\rm km\,s^{-1}}$ and $K_2 = 309.6 \pm 7.3\,{\rm km\,s^{-1}}$.

The physical properties of the system were then calculated using the JKTABSDIM code (Southworth, Maxted & Smalley 2005), which propagates uncertainties using a perturbation analysis. The distance to the system was calculated from the *UBVRI* magnitudes from Ducati et al. (2001), assuming an uncertainty of 0.02 mag on each, the JHK_s magnitudes from 2MASS (Skrutskie et al. 2006), and the bolometric corrections from Girardi et al. (2002). An interstellar extinction of $E(B-V) = 0.10 \pm 0.05$ mag was specified to bring the optical and IR distances into agreement. The resulting distance agrees well with the *Gaia* value. We find substantially smaller masses for the two stars than T07, and this can be traced to a lower value of K_2. The uncertainties in both mass and radius are dominated by the contribution from the uncertainty in K_2, and also show that the formal errors from the WD code (quoted by T07) are too small. More extensive spectroscopy of VV Ori is needed to improve its measured properties.

5 ORBITAL EVOLUTION

Orbital inclination changes have been observed in a small number of EBs; this number is growing due to the multitude of photometric surveys in operation. The list includes V907 Sco (Lacy, Helt & Vaz 1999), SS Lac (Torres 2001), HS Hya (Zasche & Paschke 2012), and systems discovered with the *Kepler* satellite (Kirk et al. 2016) and the OGLE survey (Soszyński et al. 2016).

The *TESS* light curve of VV Ori shows deep partial eclipses, but previous photometric studies have revealed the system to display obvious total eclipses (e.g. Duerbeck 1975; Eaton 1975; Chambliss & Leung 1982). To demonstrate this, we show in Fig. 2 a light curve obtained by phase binning the data obtained in the Johnson *BV* filters and the Strömgren *vby* filters by Chambliss & Leung (1982). The shapes of the two light curves clearly differ. We can rule out a problem with the *TESS* photometry because a light curve from the MASCARA survey (Burggraaff et al. 2018) shows similar partial eclipses. Our fit to the *TESS* data gives an orbital inclination of $i = 78\overset{\circ}{.}28 \pm 0\overset{\circ}{.}52$, significantly different to the values of $85\overset{\circ}{.}9 \pm 0\overset{\circ}{.}2$ found by T07 from the light curve of Chambliss & Leung (1982) and $84\overset{\circ}{.}5 \pm 0\overset{\circ}{.}5$ found by Eaton (1975) from his OAO2 data. This suggests that the orbital inclination is changing.

VV Ori benefits from a rich observational history stretching back over a century, but unfortunately none of the early light curves are easily accessible. Investigation of possible changes in i are therefore not trivial. We have found two items of evidence that the inclination was lower in the 1940s. First, Dufay (1947) presents a light curve that shows either partial or marginally total eclipses. His fit to these data, which are rather scattered, gives $i = 77\overset{\circ}{.}2$. Secondly, Huffer & Kopal (1950) state that the period of totality in primary eclipse

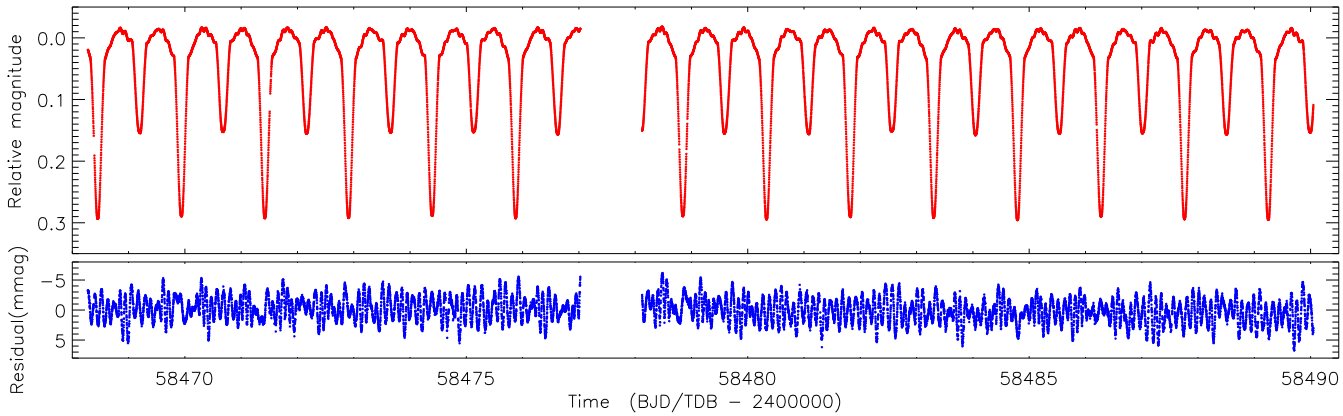

Figure 1. Top: *TESS* simple aperture photometry light curve of VV Ori. Bottom: residuals of the best JKTEBOP fit showing the pulsations.

Table 1. Brief summary of the parameters for the WD solution of the *TESS* light curve of VV Ori. Detailed descriptions of the control parameters can be found in the WD2004 user guide (Wilson & Van Hamme 2004). Uncertainties are only quoted when they account for the variation in that parameter over a full set of alternative solutions.

Parameter	Star A	Star B
Control parameters:		
WD2004 operation mode	0	
Treatment of reflection	1	
Number of reflections	1	
Limb darkening law	3 (square-root)	
Numerical grid size (normal)	60	
Numerical grid size (coarse)	40	
Fixed parameters:		
Orbital period (d)	1.485 3784	
Primary eclipse time (BJD/TDB)	2458480.33468	
Mass ratio	0.376	
Orbital eccentricity	0.0	
Rotation rates	1.0	1.0
Bolometric albedos	1.0	1.0
Gravity darkening	1.0	1.0
Bolometric linear LD coefficients	0.6288	0.7121
Linear LD coefficient	−0.1188	−0.0612
Square-root LD coefficient	0.4694	0.4073
Fitted parameters:		
Orbital inclination (°)	78.28 ± 0.52	
Third light	0.005 ± 0.069	
Light contributions	11.24 ± 0.88	1.299 ± 0.069
Potentials	3.132 ± 0.028	3.397 ± 0.102
Derived parameters:		
Fractional radii	0.3718 ± 0.0010	0.1817 ± 0.0034
Orbital separation ($R_\odot$)	13.51 ± 0.05	
Mass ($M_\odot$)	9.52 ± 0.56	3.80 ± 0.16
Radius ($R_\odot$)	4.958 ± 0.088	2.360 ± 0.061
Log surface gravity (cgs)	4.026 ± 0.011	4.272 ± 0.018
$T_{\rm eff}$ (K)	26 200 ± 1000	16 100 ± 1000
Log luminosity ($L_\odot$)	4.02 ± 0.07	2.53 ± 0.11
Absolute bolometric magnitude	−5.36 ± 0.17	−1.65 ± 0.27
Distance (pc)	371 ± 12	

lasts for 0.042 ± 0.003 phase units. Our by-eye measurement of the duration of totality in the Chambliss & Leung (1982) light curves is 0.060 ± 0.005 in phase units.

Due to the symmetry inherent in spatially unresolved two-body motion, the light curves of EBs have no indication of whether i is above or below 90°, so by convention inclinations are quoted as the smaller of i or $(90^\circ - i)$. We therefore suggest that VV Ori is undergoing orbital precession that manifests as a change in i, that it used to show partial eclipses, that the inclination rose to the maximum of $i = 90^\circ$ some time in the 1950s or 1960s, and is now decreasing by approximately 0.2° yr^{-1}. Using WD2004, we find that the lower limit for eclipses to occur in this system is 56.8°. When – or if – VV Ori will cease to eclipse in the future will be investigated in detail in a future work. One other relevant constraint is that the binarity of the system was discovered through visual observations of its photometic variability in 1903 (Barr 1905). This almost certainly

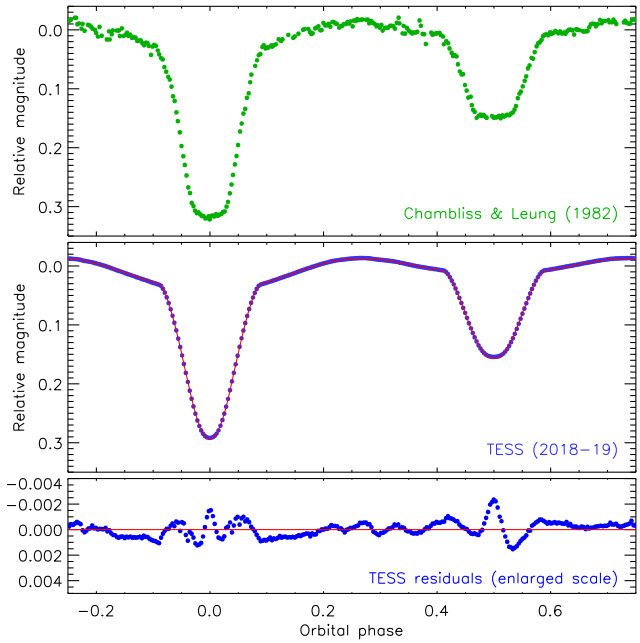

Figure 2. Top: light curve from Chambliss & Leung (1982) obtained by phase binning the *BV* and *vby* data together. Middle: phase-binned light curve of VV Ori (filled blue circles) with the best fit from the WD code (red solid line). Bottom: residuals of the fit to the *TESS* data.

indicates it was eclipsing at this time because the amplitude of the proximity effects in this system is very low for visual observations: roughly 0.04 mag at $i = 60^\circ$.

6 PULSATION ANALYSIS

To examine the pulsational properties of VV Ori, we subtracted a multifrequency harmonic model of the orbital frequency, $\nu_{\rm orb} = 0.673\,229 \pm 0.000\,001$ d^{-1}, from the light curve and calculated a residual amplitude spectrum using a discrete Fourier transform (Kurtz 1985). We employed iterative pre-whitening to extract all significant frequencies using the standard amplitude signal-to-noise (S/N) criterion of Breger (1993), such that significant frequencies have S/N $\geq$ 4. The S/N of each peak was calculated using its amplitude and the average amplitude within a 1 d^{-1} window at the location of the extracted frequency. In total, we extracted 51 significant frequencies between 1.4 and 27.8 d^{-1}. The frequencies, amplitudes, and phases and their corresponding 1σ uncertainties were obtained from a multifrequency non-linear least-squares fit to the light curve (Kurtz et al. 2015; Bowman 2017), and are provided in Table A1. The amplitude spectra before and after pre-whitening all significant pulsation modes are shown in Fig. 3.

VV Ori exhibits two multiplets of pulsation modes split by the orbital frequency (centred at $\nu_1 = 9.1766 \pm 0.0001$ and $\nu_2 = 9.0324 \pm 0.0002$ d^{-1}), as indicated in Fig. 3, and several additional pulsation frequencies. Given the frequencies of the two dominant modes, ν_1 and ν_2, we attribute them to the β Cep primary. In slowly rotating pulsators, symmetric frequency multiplets are plausible (see Bowman 2020). However, the inferred rotation rate assuming ν_1 and ν_2 as the retrograde and prograde components of a non-radial mode would imply an uncommonly slow rotation rate for such a massive star. On the other hand, such multiplets are the signature of tidally perturbed modes (Bowman et al. 2019; Bowman 2020; Jerzykiewicz et al. 2020; Southworth et al. 2020), amplitude modulation during the orbit caused by a changing light ratio, and tidally tilted pulsators (Fuller et al. 2020; Handler et al. 2020; Kurtz et al. 2020). Our analysis reveals that the pulsation amplitudes are not maximal at a specific orbital phase (see Fig. 1). Hence, if VV Ori is a tidally tilted pulsator, it is different to those studied by Handler et al. (2020) and Kurtz et al. (2020).

There are several independent g-mode frequencies below 3 d^{-1}, which we suggest arise from the less-massive secondary star, making it a possible SPB star. We also find that the high-frequency doublets (shown in yellow in Fig. 3) can be explained by high-order combination frequencies of the orbital frequency and the two dominant modes ν_1 and ν_2 [e.g. $\nu_1 + \nu_2 + n\,\nu_{\rm orb}$, where $n \in (6, 8, 10)$]. The remaining significant frequencies are shown in green in Fig. 3, and we interpret these as independent given that only high-order coincidental combination relations are possible. In Table A1, we provide the identifications of the extracted frequencies. Additional 'missing' component frequencies of the multiplets can clearly be seen in Fig. 3, but these fall below our S/N criterion.

At the suggestion of the referee, we investigated whether imperfections in the binary modelling (Section 3) could have affected the pulsation frequencies we have identified in VV Ori. To do this, we generated a set of slightly different models of the *TESS* light curve using JKTEBOP, by ignoring third light, or fitting for $e\cos\omega$, or fixing the sum of the fractional radii of the stars to a value 4σ smaller than the fitted value, or changing the mass ratio and thus the shapes of the stars. The frequency spectra of these data sets show differences at the orbital harmonics, but the pulsation multiplets we find are essentially unaffected. This shows that our pulsation analysis is robust against changes in the modelling of binarity, and that the multiplets are not methodological in origin.

7 SUMMARY AND DISCUSSION

VV Ori is an early-type binary system containing a 9.5 and 3.8 $M_\odot$ star on a short-period orbit. It used to have total eclipses but the *TESS* photometry shows that these eclipses are now partial. We have fitted the *TESS* light curve and published RVs, and determined the physical properties of the stars. The orbital inclination is significantly lower than found in previous studies, and this change is probably driven by dynamical interactions with a third body. Together with the directly imaged companion at an angular separation of 0.23 arcsec, this means that the VV Ori system is at least quadruple.

The *TESS* data reveal 51 significant frequencies, including independent g- and p-mode pulsations. We interpret the p-mode pulsations as arising from the primary star, making VV Ori A the second β Cephei star in an EB with a precisely measured mass (after V453 Cyg A; Southworth et al. 2020). The g-mode pulsations possibly originate from the secondary star, in which case VV Ori B is the second known SPB star in an EB (after V539 Ara B; Clausen 1996). Two frequency multiplets of the dominant p modes with a spacing of the orbital frequency are also evident. The equilibrium tide in short-period circular binaries can give rise to a spheroidal bulge and ellipsoidal variability, but is also predicted to perturb self-excited non-radial pulsations and produce such pulsation frequency multiplets (Reyniers & Smeyers 2003; Balona 2018). Such multiplets of pulsation modes have recently been detected in a handful of short-period EBs (Bowman et al. 2019; Fuller et al. 2020; Handler et al. 2020; Jerzykiewicz et al. 2020; Kurtz et al. 2020; Southworth et al. 2020).

The multiperiodic frequency spectrum makes VV Ori a prime target for future asteroseismic modelling (see Schmid & Aerts 2016; Johnston et al. 2019). Furthermore, such pulsating stars in

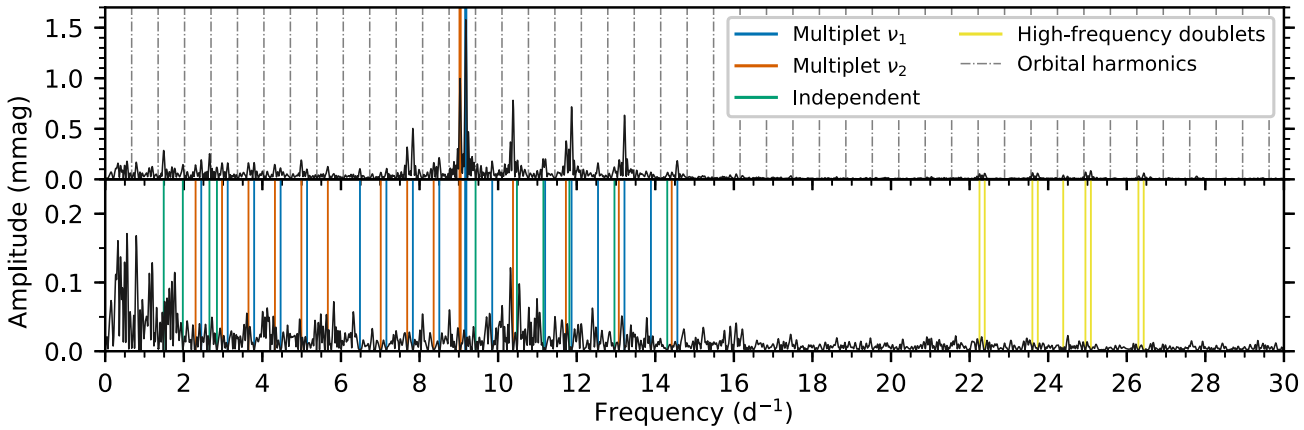

Figure 3. Amplitude spectra of VV Ori after removal of the binary model (top), and after removal of the significant pulsation frequencies too (bottom). The location and identity of extracted frequencies are shown as coloured lines, and the dashed grey lines represent harmonics of the orbital frequency.

EBs open up new avenues to perform tidal asteroseismology and inspect the currently mysterious interiors of massive stars. In the near future, VV Ori will be re-observed using *TESS*, giving a new data set to further refine the asteroseismic analysis and study the orbital evolution of the system. We have also begun a spectroscopic campaign on this system with the aim of measuring masses and $T_{\rm eff}$ values to higher precision, and detecting and identifying line-profile variability due to the pulsations in both components.

ACKNOWLEDGEMENTS

We thank Gerald Handler and two referees for helpful comments on the manuscript. The *TESS* data presented in this paper were obtained from the Mikulski Archive for Space Telescopes (MAST) at the Space Telescope Science Institute (STScI). STScI is operated by the Association of Universities for Research in Astronomy, Inc. Support to MAST for these data is provided by the NASA Office of Space Science. Funding for the *TESS* mission is provided by the NASA Explorer Program. The research leading to these results has received funding from the Research Foundation Flanders (FWO) by means of a senior postdoctoral fellowship with grant agreement no. 1286521N, and from the European Research Council (ERC) under the European Union's Horizon 2020 research and innovation programme (grant agreement no. 670519: MAMSIE).

DATA AVAILABILITY

All data underlying this article are available in the MAST archive (https://mast.stsci.edu/portal/Mashup/Clients/Mast/Portal.html) and from Terrell et al. (2007).

REFERENCES

Aerts C., Thoul A., Daszyńska J., Scuflaire R., Waelkens C., Dupret M. A., Niemczura E., Noels A., 2003, Science, 300, 1926
Aerts C., Christensen-Dalsgaard J., Kurtz D. W., 2010, Asteroseismology. Astronomy and Astrophysics Library. Springer-Verleg, Amsterdam, Berlin
Aerts C., Mathis S., Rogers T. M., 2019, ARA&A, 57, 35
Andersen J., 1991, Astron. Astrophys. Rev., 3, 91
Balona L. A., 2018, MNRAS, 476, 4840
Barr J. M., 1905, Proc. R. Astron. Soc. Can., 42
Bowman D. M., 2017, Amplitude Modulation of Pulsation Modes in Delta Scuti Stars, Springer Theses series. Springer, US
Bowman D. M., 2020, Astronomy and Space Sciences, 7, 70
Bowman D. M., Johnston C., Tkachenko A., Mkrtichian D. E., Gunsriwiwat K., Aerts C., 2019, ApJ, 883, L26
Breger M., 1993, Ap&SS, 210, 173
Briquet M., Morel T., Thoul A., Scuflaire R., Miglio A., Montalbán J., Dupret M. A., Aerts C., 2007, MNRAS, 381, 1482
Briquet M., Neiner C., Leroy B., Pápics P. I., MiMeS Collaboration, 2013, A&A, 557, L16
Burggraaff O. et al., 2018, A&A, 617, A32
Burssens S. et al., 2020, A&A, 639, A81
Chambliss C. R., Leung K. C., 1982, ApJS, 49, 531
Claret A., Torres G., 2018, ApJ, 859, 100
Clausen J. V., 1996, A&A, 308, 151
Daniel Z., 1916, Publ. Allegheny Obs. Pittsburgh, 3, 179
Ducati J. R., Bevilacqua C. M., Rembold S. B., Ribeiro D., 2001, ApJ, 558, 309
Duerbeck H. W., 1975, A&AS, 22, 19
Dufay J., 1947, Ann. Astrophys., 10, 158
Eaton J. A., 1975, ApJ, 197, 379
Fuller J., 2017, MNRAS, 472, 1538
Fuller J., Kurtz D. W., Handler G., Rappaport S., 2020, MNRAS, 498, 5730
Gaia Collaboration, 2018, A&A, 616, A1
Girardi L., Bertelli G., Bressan A., Chiosi C., Groenewegen M. A. T., Marigo P., Salasnich B., Weiss A., 2002, A&A, 391, 195
Hambleton K. M. et al., 2013, MNRAS, 434, 925
Handler G. et al., 2020, Nat. Astron., 4, 684
Horch E. P. et al., 2017, AJ, 153, 212
Huffer C. M., Kopal Z., 1950, AJ, 55, 171
Law N. M., Dekany R. G., Mackay C. D., Moore A. M., Britton M. C., Velur V., 2008, in Hubin N., Max C. E., Wizinowich P. L., eds, Proc. SPIE Conf. Ser., 7015, Adaptive Optics Systems. SPIE, Bellingham, p. 701521
Jerzykiewicz M., Pigulski A., Handler G., Moffat A. F. J., Popowicz A., Wade G. A., Zwintz K., Pablo H., 2020, MNRAS, 496, 2391
Johnston C., Tkachenko A., Aerts C., Molenberghs G., Bowman D. M., Pedersen M. G., Buysschaert B., Pápics P. I., 2019, MNRAS, 482, 1231
Kirk B. et al., 2016, AJ, 151, 68
Kurtz D. W., 1985, MNRAS, 213, 773
Kurtz D. W., Shibahashi H., Murphy S. J., Bedding T. R., Bowman D. M., 2015, MNRAS, 450, 3015
Kurtz D. W. et al., 2020, MNRAS, 494, 5118
Lacy C. H. S., Helt B. E., Vaz L. P. R., 1999, AJ, 117, 541
Langer N., 2012, ARA&A, 50, 107
Lesh J. R., Aizenman M. L., 1978, ARA&A, 16, 215
Maxted P. F. L. et al., 2020, MNRAS, 498, 332
Pedersen M. G. et al., 2019, ApJ, 872, L9
Pietrzyński G. et al., 2019, Nature, 567, 200

Ratajczak M., Pigulski A., Pavlovski K., 2017, in Zwintz K., Poretti E., eds, Second BRITE – Constellation Science Conference: Small Satellites - Big Science Vol. 5, Polish Astronomical Society, Warsaw. p. 128
Reyniers K., Smeyers P., 2003, A&A, 404, 1051
Ricker G. R. et al., 2015, J. Astron. Telesc. Inst. Syst., 1, 014003
Sana H. et al., 2012, Science, 337, 444
Sarma M. B. K., Vivekananda Rao P., 1995, J. Astrophys. Astron., 16, 407
Schmid V. S., Aerts C., 2016, A&A, 592, A116
Skrutskie M. F. et al., 2006, AJ, 131, 1163
Soszyński I. et al., 2016, Anal. Chim. Acta, 66, 405
Southworth J., 2008, MNRAS, 386, 1644
Southworth J., Maxted P. F. L., Smalley B., 2005, A&A, 429, 645
Southworth J. et al., 2011, MNRAS, 414, 2413
Southworth J., Bowman D., Tkachenko A., Pavlovski K., 2020, MNRAS, 497, L19
Stankov A., Handler G., 2005, ApJS, 158, 193
Struve O., Luyten W. J., 1949, ApJ, 110, 160
Terrell D., Munari U., Siviero A., 2007, MNRAS, 374, 530
Tkachenko A. et al., 2020, A&A, 637, A60
Torres G., 2001, AJ, 121, 2227
Torres G., Andersen J., Giménez A., 2010, Astron. Astrophys. Rev., 18, 67
Van Hamme W., 1993, AJ, 106, 2096
Van Hamme W., Wilson R. E., 2007, ApJ, 661, 1129
Waelkens C., 1991, A&A, 246, 453
Welsh W. F. et al., 2011, ApJS, 197, 4
Wilson R. E., Devinney E. J., 1971, ApJ, 166, 605
Wilson R. E., Van Hamme W., 2004, Computing Binary Star Observables (Wilson-Devinney Program User Guide)
Wood F. B., 1946, Contr. Princeton Univ. Obs., 21, 1
Zasche P., Paschke A., 2012, A&A, 542

SUPPORTING INFORMATION

Supplementary data are available at *MNRASL* online.

Table S1. Frequencies, amplitudes, and phases of significant frequencies in VVOri.

Please note: Oxford University Press is not responsible for the content or functionality of any supporting materials supplied by the authors. Any queries (other than missing material) should be directed to the corresponding author for the article.

This paper has been typeset from a TEX/LATEX file prepared by the author.

List of astronomical key words (Updated on 2020 January)

This list is common to *Monthly Notices of the Royal Astronomical Society, Astronomy and Astrophysics*, and *The Astrophysical Journal*. In order to ease the search, the key words are subdivided into broad categories. No more than *six* subcategories altogether should be listed for a paper.

The subcategories in boldface containing the word 'individual' are intended for use with specific astronomical objects; these should never be used alone, but always in combination with the most common names for the astronomical objects in question. Note that each object counts as one subcategory within the allowed limit of six.

The parts of the key words in italics are for reference only and should be omitted when the keywords are entered on the manuscript.

General
editorials, notices
errata, addenda
extraterrestrial intelligence
history and philosophy of astronomy
miscellaneous
obituaries, biographies
publications, bibliography
sociology of astronomy
standards

Physical data and processes
acceleration of particles
accretion, accretion discs
asteroseismology
astrobiology
astrochemistry
astroparticle physics
atomic data
atomic processes
black hole physics
chaos
conduction
convection
dense matter
diffusion
dynamo
elementary particles
equation of state
gravitation
gravitational lensing: micro
gravitational lensing: strong
gravitational lensing: weak
gravitational waves
hydrodynamics
instabilities
line: formation
line: identification
line: profiles
magnetic fields
magnetic reconnection
(magnetohydrodynamics) MHD
masers
molecular data
molecular processes
neutrinos
nuclear reactions, nucleosynthesis, abundances
opacity
plasmas
polarization
radiation: dynamics
radiation mechanisms:general
radiation mechanisms: non-thermal
radiation mechanisms: thermal
radiative transfer
relativistic processes
scattering
shock waves
solid state: refractory
solid state: volatile
turbulence
waves

Astronomical instrumentation, methods and techniques
atmospheric effects
balloons
instrumentation: adaptive optics
instrumentation: detectors
instrumentation: high angular resolution
instrumentation: interferometers
instrumentation: miscellaneous
instrumentation: photometers
instrumentation: polarimeters
instrumentation: spectrographs
light pollution
methods: analytical
methods: data analysis
methods: laboratory: atomic
methods: laboratory: molecular
methods: laboratory: solid state
methods: miscellaneous
methods: numerical
methods: observational
methods: statistical
site testing
space vehicles
space vehicles: instruments
techniques: high angular resolution
techniques: image processing
techniques: imaging spectroscopy
techniques: interferometric
techniques: miscellaneous
techniques: photometric
techniques: polarimetric
techniques: radar astronomy
techniques: radial velocities
techniques: spectroscopic
telescopes

Astronomical data bases
astronomical data bases: miscellaneous
atlases
catalogues
surveys
virtual observatory tools

Software
software: data analysis
software: development
software: documentation
software: public release
software: simulations

Astrometry and celestial mechanics
astrometry
celestial mechanics
eclipses
ephemerides
occultations
parallaxes
proper motions
reference systems
time

The Sun
Sun: abundances
Sun: activity
Sun: atmosphere
Sun: chromosphere
Sun: corona
Sun: coronal mass ejections (CMEs)
Sun: evolution
Sun: faculae, plages
Sun: filaments, prominences
Sun: flares
Sun: fundamental parameters
Sun: general
Sun: granulation
Sun: helioseismology
Sun: heliosphere
Sun: infrared
Sun: interior
Sun: magnetic fields
Sun: oscillations
Sun: particle emission
Sun: photosphere
Sun: radio radiation
Sun: rotation
(Sun:) solar–terrestrial relations
(Sun:) solar wind
(Sun:) sunspots
Sun: transition region
Sun: UV radiation
Sun: X-rays, gamma-rays

Planetary systems
comets: general

comets: individual: . . .
Earth
interplanetary medium
Kuiper belt: general

Kuiper belt objects: individual: . . .
meteorites, meteors, meteoroids
minor planets, asteroids: general
minor planets, asteroids: individual: . . .
Moon
Oort Cloud
planets and satellites: atmospheres
planets and satellites: aurorae
planets and satellites: composition
planets and satellites: detection
planets and satellites: dynamical evolution and stability
planets and satellites: formation
planets and satellites: fundamental parameters
planets and satellites: gaseous planets
planets and satellites: general

planets and satellites: individual: . . .
planets and satellites: interiors
planets and satellites: magnetic fields
planets and satellites: oceans
planets and satellites: physical evolution
planets and satellites: rings
planets and satellites: surfaces
planets and satellites: tectonics
planets and satellites: terrestrial planets
planet–disc interactions
planet–star interactions
protoplanetary discs
zodiacal dust

Stars
stars: abundances
stars: activity
stars: AGB and post-AGB
stars: atmospheres
(stars:) binaries *(including multiple)*: close
(stars:) binaries: eclipsing
(stars:) binaries: general
(stars:) binaries: spectroscopic
(stars:) binaries: symbiotic
(stars:) binaries: visual
stars: black holes
(stars:) blue stragglers
(stars:) brown dwarfs
stars: carbon
stars: chemically peculiar
stars: chromospheres
(stars:) circumstellar matter
stars: coronae
stars: distances
stars: dwarf novae
stars: early-type
stars: emission-line, Be
stars: evolution
stars: flare
stars: formation
stars: fundamental parameters
(stars:) gamma-ray burst: general
(stars:) **gamma-ray burst: individual: . . .**
stars: general
(stars:) Hertzsprung–Russell and colour–magnitude diagrams
stars: horizontal branch
stars: imaging
stars: individual: . . .
stars: interiors

stars: jets
stars: kinematics and dynamics
stars: late-type
stars: low-mass
stars: luminosity function, mass function
stars: magnetars
stars: magnetic field
stars: massive
stars: mass-loss
stars: neutron
(stars:) novae, cataclysmic variables
stars: oscillations *(including pulsations)*
stars: peculiar *(except chemically peculiar)*
(stars:) planetary systems
stars: Population II
stars: Population III
stars: pre-main-sequence
stars: protostars
(stars:) pulsars: general
(stars:) **pulsars: individual: . . .**
stars: rotation
stars: solar-type
(stars:) starspots
stars: statistics
(stars:) subdwarfs
(stars:) supergiants
(stars:) supernovae: general
(stars:) **supernovae: individual: . . .**
stars: variables: Cepheids
stars: variables: Scuti
stars: variables: general
stars: variables: RR Lyrae
stars: variables: S Doradus
stars: variables: T Tauri, Herbig Ae/Be
(stars:) white dwarfs
stars: winds, outflows
stars: Wolf–Rayet

Interstellar medium (ISM), nebulae
ISM: abundances
ISM: atoms
ISM: bubbles
ISM: clouds
(ISM:) cosmic rays
(ISM:) dust, extinction
ISM: evolution
ISM: general
(ISM:) HII regions
(ISM:) Herbig–Haro objects

ISM: individual objects: . . .
(except planetary nebulae)
ISM: jets and outflows
ISM: kinematics and dynamics
ISM: lines and bands
ISM: magnetic fields
ISM: molecules
(ISM:) photodissociation region (PDR)
(ISM:) planetary nebulae: general
(ISM:) **planetary nebulae: individual: . . .**
ISM: structure
ISM: supernova remnants

The Galaxy
Galaxy: abundances
Galaxy: bulge
Galaxy: centre
Galaxy: disc
Galaxy: evolution
Galaxy: formation
Galaxy: fundamental parameters
Galaxy: general
(Galaxy:) globular clusters: general
(Galaxy:) **globular clusters: individual: . . .**
Galaxy: halo
Galaxy: kinematics and dynamics
(Galaxy:) local interstellar matter
Galaxy: nucleus
(Galaxy:) open clusters and associations: general
(Galaxy:) **open clusters and associations: individual: . . .**
(Galaxy:) solar neighbourhood
Galaxy: stellar content
Galaxy: structure

Galaxies
galaxies: abundances
galaxies: active
galaxies: bar
(galaxies:) BL Lacertae objects: general
(galaxies:) **BL Lacertae objects: individual: . . .**
galaxies: bulges
galaxies: clusters: general

galaxies: clusters: individual: . . .
galaxies: clusters: intracluster medium
galaxies: disc
galaxies: distances and redshifts
galaxies: dwarf
galaxies: elliptical and lenticular, cD
galaxies: evolution
galaxies: formation
galaxies: fundamental parameters
galaxies: general
galaxies: groups: general

galaxies: groups: individual: . . .
galaxies: haloes
galaxies: high-redshift

galaxies: individual: . . .
galaxies: interactions
(galaxies:) intergalactic medium
galaxies: irregular
galaxies: ISM
galaxies: jets
galaxies: kinematics and dynamics
(galaxies:) Local Group
galaxies: luminosity function, mass function
(galaxies:) Magellanic Clouds
galaxies: magnetic fields
galaxies: nuclei
galaxies: peculiar
galaxies: photometry
(galaxies:) quasars: absorption lines
(galaxies:) quasars: emission lines
(galaxies:) quasars: general

(galaxies:) **quasars: individual: . . .**
(galaxies:) quasars: supermassive black holes
galaxies: Seyfert
galaxies: spiral
galaxies: starburst
galaxies: star clusters: general

galaxies: star clusters: individual: . . .
galaxies: star formation
galaxies: statistics
galaxies: stellar content
galaxies: structure

Cosmology
(cosmology:) cosmic background radiation
(cosmology:) cosmological parameters
(cosmology:) dark ages, reionization, first stars
(cosmology:) dark energy
(cosmology:) dark matter
(cosmology:) diffuse radiation
(cosmology:) distance scale
(cosmology:) early Universe
(cosmology:) inflation
(cosmology:) large-scale structure of Universe
cosmology: miscellaneous
cosmology: observations
(cosmology:) primordial nucleosynthesis
cosmology: theory

Resolved and unresolved sources as a function of wavelength
gamma-rays: diffuse background
gamma-rays: galaxies
gamma-rays: galaxies: clusters
gamma-rays: general
gamma-rays: ISM
gamma-rays: stars
infrared: diffuse background
infrared: galaxies
infrared: general
infrared: ISM
infrared: planetary systems
infrared: stars
radio continuum: galaxies
radio continuum: general
radio continuum: ISM
radio continuum: planetary systems
radio continuum: stars
radio continuum: transients
radio lines: galaxies
radio lines: general
radio lines: ISM
radio lines: planetary systems
radio lines: stars
submillimetre: diffuse background
submillimetre: galaxies
submillimetre: general
submillimetre: ISM
submillimetre: planetary systems
submillimetre: stars
ultraviolet: galaxies
ultraviolet: general
ultraviolet: ISM
ultraviolet: planetary systems
ultraviolet: stars
X-rays: binaries
X-rays: bursts
X-rays: diffuse background
X-rays: galaxies
X-rays: galaxies: clusters
X-rays: general
X-rays: individual: . . .
X-rays: ISM
X-rays: stars

Transients
(transients:) black hole mergers
(transients:) black hole - neutron star mergers
(transients:) fast radio bursts
(transients:) gamma-ray bursts
(transients:) neutron star mergers
transients: novae
transients: supernovae
transients: tidal disruption events